

Signatures of electronic correlations in iron silicide

Jan M. Tomczak¹, Kristjan Haule, and Gabriel Kotliar

Department of Physics and Astronomy, Rutgers University, Piscataway, NJ 08854

Edited by* Elihu Abrahams, University of California, Los Angeles, CA, and approved January 3, 2012 (received for review November 7, 2011)

The intermetallic FeSi exhibits an unusual temperature dependence in its electronic and magnetic degrees of freedom, epitomized by the cross-over from a low-temperature nonmagnetic semiconductor to a high-temperature paramagnetic metal with a Curie–Weiss-like susceptibility. Many proposals for this unconventional behavior have been advanced, yet a consensus remains elusive. Using realistic many-body calculations, we here reproduce the signatures of the metal-insulator cross-over in various observables: the spectral function, the optical conductivity, the spin susceptibility, and the Seebeck coefficient. Validated by quantitative agreement with experiment, we then address the underlying microscopic picture. We propose a new scenario in which FeSi is a band insulator at low temperatures and is metalized with increasing temperature through correlation induced incoherence. We explain that the emergent incoherence is linked to the unlocking of iron fluctuating moments, which are almost temperature independent at short timescales. Finally, we make explicit suggestions for improving the thermoelectric performance of FeSi based systems.

strongly correlated electrons | Kondo insulator | metal-insulator transitions | electronic structure | material science

Iron-based narrow gap semiconductors such as FeSi, FeSb₂, or FeGa₃ show a pronounced resemblance to heavy fermion Kondo insulators in their charge (1–4) and spin (4, 5) degrees of freedom. Besides, these systems display a large thermopower (1, 3, 6–9), heralding their potential use in solid-state devices. There are two complementary approaches for explaining these unusual properties: On one hand, it has been proposed that lattice degrees of freedom play a crucial role (7, 10, 11). On the other hand, electron–electron correlation effects have been invoked on the basis of both experimental results (2–4, 8), as well as theoretical model studies (12–15), advocating, in particular, Hubbard physics (12, 14, 15), spin fluctuations (13), spin-state transitions (16, 17), or a thermally induced mixed valence (18).

Here, we go beyond modelistic approaches and investigate the effect of correlations on prototypical FeSi from the *ab initio* perspective. The key issues that we address are (i) can electronic Coulomb correlations alone quantitatively account for the signatures of the temperature induced cross-over in various observables, and (ii) what is the underlying microscopic origin of this behavior? As a realistic many-body approach, we employ the combination of density functional theory (DFT) and dynamical mean-field theory (DMFT), DFT + DMFT (for a review see, e.g., ref. 19) as implemented in ref. 20. For the calculation of the Seebeck coefficient, we have extended our previous work (9) for DFT computations to include the DMFT self-energy in a full orbital setup. For details, see *SI Text*.

At low temperatures, iron silicide is a semiconductor with a gap $\Delta \approx 50$ –60 meV (2, 5, 21), with the resistivity (1, 6) and the magnetic susceptibility (5) following activation laws. At 150–200 K (i.e., at temperatures much smaller than Δ) a cross-over to a (bad) metal is observed in transport (1, 6, 22) and optical spectroscopy (2, 17, 21–24). Moreover, FeSi displays a maximum in the susceptibility at 400 K, followed by a Curie–Weiss-like law (5). The energy scale over which spectral weight in the optical conductivity is transferred through the transition has been long debated (2, 17, 21, 22). Recent ellipsometry measurements (24) showed that weight is moved over several electronvolts—

a common harbinger of correlation effects (25). The Seebeck coefficient of FeSi peaks near 50 K with a remarkable 700 $\mu\text{V}/\text{K}$, but is quickly suppressed at higher temperatures, when the unusual spin and charge properties set in (1, 6, 7).

Spectral Properties

Fig. 1 shows our theoretical local spectral function of FeSi at various temperatures (orbital and momentum resolved spectra can be found in the *SI Text*). At low temperature, the spectrum is similar to that obtained within band theory (10, 14, 26), albeit with a gap renormalized by a factor of about two, in agreement with photoemission spectroscopy (PES) (27, 28).[†] The electronic excitation spectrum is thus band-like and coherent at low temperature. As was noted earlier (10, 14, 26), the gap edges are very sharp in this regime, indicating a potentially large thermopower (29). At higher temperatures, features broaden and the system becomes a bad metal as found experimentally (27, 28). We stress that this effect is largely beyond a mere temperature broadening of the electron distribution (Fermi) function (2, 27, 28). Because of the asymmetry of the spectrum, the position of the gap moves with temperature: In agreement with PES (27, 28), the minimum ω_{\min} of the spectrum (depicted in Fig. 1) starts out near the middle of the gap (as expected for a semiconductor; ref. 9), then first moves up with increasing temperature. Above 300 K, ω_{\min} again approaches the Fermi level as the asymmetry is reversed.

Optical Spectroscopy

Owing to a high precision and the existence of sum-rule arguments, optical spectroscopy is a valuable tool for tracking the evolution of a system under change of external parameters. Transfers of spectral weight over scales related to the Coulomb interaction U rather than the gap Δ are usually considered a hallmark of correlation effects (25). Recent ellipsometry measurements (24) showed spectral weight transfers over several electronvolts. In Fig. 2, we compare our realistic optical conductivities $\sigma(\omega, T)$ to experiment (23, 24). Both the overall magnitude and the crucial temperature evolution are well captured: Cooling down from 400 K depletes spectral weight below 80 meV, with only parts of it being transferred to energies just slightly above the gap. To analyze this in more detail, we follow Menzel et al. (24) and plot in Fig. 3 the temperature difference $\Delta N(\omega) = N_{T_1}(\omega) - N_{T_2}(\omega)$ of the effective number of carriers $N_T(\omega) = \frac{2m_e V}{\pi e^2} \int_0^\omega d\omega' \sigma(\omega', T)$ as a function of energy. An intersection with the x axis corresponds to a full recovery of spectral weight as is imposed by the f -sum rule. Our theoretical results quantitatively trace the experimental temperature dependence. We note that there are several isosbestic points in the optical conductivity, Fig. 2, which lead to extrema in $\Delta N(\omega)$ in Fig. 3. The first peak in ΔN is at 80 meV, the scale of the semiconducting gap, above which spectral weight starts to pile

Author contributions: J.M.T. designed research; J.M.T. performed research; J.M.T. developed *ab initio* thermoelectric power algorithms and codes; J.M.T. carried out computations; J.M.T., K.H., and G.K. analyzed data; and J.M.T., K.H., and G.K. wrote the paper.

The authors declare no conflict of interest.

*This Direct Submission article had a prearranged editor.

[†]From the slope of the self-energy Σ , we extract $m^* / m = 1.5$; the rest of the gap shrinking comes from interorbital shifts as induced by the real parts of the self-energy $\Re \Sigma(0)$.

[‡]To whom correspondence should be addressed. E-mail: jtomczak@physics.rutgers.edu.

This article contains supporting information online at www.pnas.org/lookup/suppl/doi:10.1073/pnas.1118371109/-DCSupplemental.

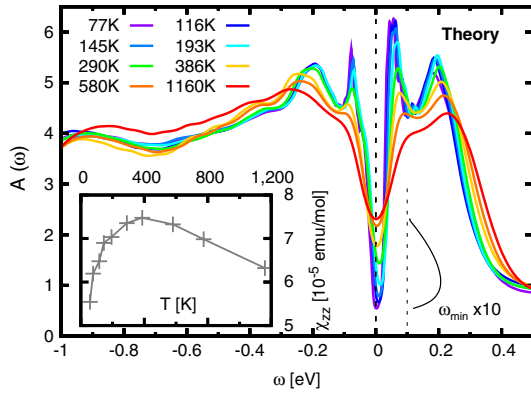


Fig. 1. Local spectra and susceptibility. The theoretical local spectral function for different temperatures. The spectral minimum with respect to the Fermi level ($10\times$ magnified) is traced by ω_{\min} . (Inset) Local spin susceptibility.

up at low temperature in $\sigma(\omega)$. The first minimum in $\Delta N(\omega)$ occurs at the second isosbestic point at around 0.18 eV, up to where only approximately 35% compensation of excess carriers is achieved for the theoretical curve. As is clear from Fig. 3, $\Delta N(\omega)$ does not vanish over the extended energy range plotted, hence a total compensation is not reached below the scale of the Coulomb repulsion of 5 eV. As a further assessment, we show, in Fig. 44, the theoretical resistivity in comparison with several experiments.

Thermopower

FeSi boasts a notably large thermopower at low temperatures (1, 6, 7), yet its magnitude is compatible with a Seebeck coefficient of purely electronic origin: For a band-like semiconductor in the regime $k_B T < \Delta$, the electron diffusive thermopower cannot exceed Δ/T (9). From this perspective, a larger gap favors the thermopower. Although validated in FeSi, the above constraint is violated in the related compound FeSb₂ (3, 8, 9). Given the dominantly electronic picture, in conjunction with the band-like nature of FeSi at low temperature, the Seebeck coefficient in that regime can be accounted for by band theory: Indeed, it was shown that a slightly hole doped band-structure yields good agreement below 100 K (10). As shown in Fig. 5, we confirm this by supplementing band theory with an effective mass of 2 and 0.001 holes/Fe. Although a dependence on stoichiometry is seen in experiments (6), the tiny amounts of extra holes should be viewed as a means to alter the particle-hole asymmetry (9) rather than an effect of excess charge. As is well known, the particle-hole asymmetry plays a major role in determining the thermopower because electron and hole contributions have opposite signs.

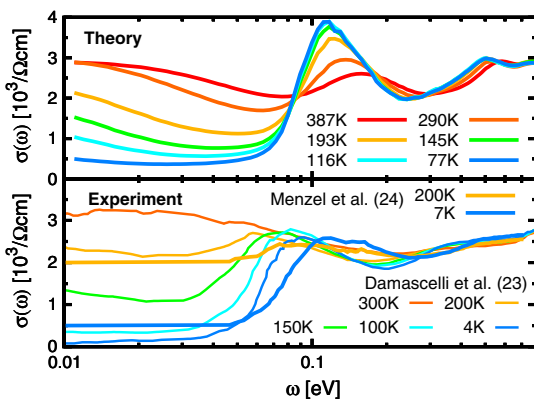


Fig. 2. Optical conductivity. Theoretical (Upper) and experimental (23, 24) (Lower) optical conductivity as a function of frequency for various temperatures.

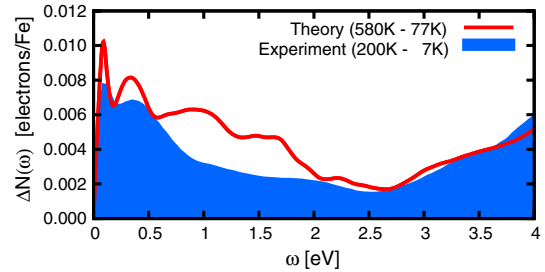


Fig. 3. Transfer of spectral weight. Difference of high- and low-temperature carrier density as obtained from the integrated spectral weight (see text for details). Experimental results from ref. 24, used temperatures as indicated.

The convention is that a negative Seebeck coefficient is dominated by electron transport, and a positive one by holes. It is interesting to note that, for an insulator, a large thermopower is expected *near* thermoelectric particle/hole symmetry (9), with a large sensitivity to the exact imbalance of carriers. Scanning through electron and hole doping, FeSi is experimentally indeed placed near such a boundary (30).

As expected, introducing an effective mass alone fails at higher temperatures. It has been conjectured (but not calculated) that this could be accounted for by thermal disorder via the electron-phonon coupling (10, 11). On the other hand, model studies indicated compatibility with the picture of Coulomb correlations (31). In Fig. 5, we display the Seebeck coefficient obtained from our realistic many-body calculation. The agreement with experiments is very good. Notably, the theory captures the overall suppression of the thermopower above 100 K, which comes from an enhanced conductivity due to the accumulation of incoherent weight at the Fermi level. In this sense, incoherence is detrimental to semiconductor-based thermopower. Note, however, that correlation effects can substantially enhance the Seebeck coefficient of correlated metals (see, e.g., ref. 32).

The temperature dependence of the Seebeck coefficient in Fig. 5 is connected to the moving of the chemical potential discussed above: As a function of rising temperature, the chemical potential first moves down, thereby increasing the electron contribution to the thermopower (9). At some temperature, thermoelectric particle-hole symmetry is passed and the Seebeck coefficient is dominated by electrons ($S < 0$), whereas at higher temperatures, the trend is reversed and S becomes positive again.

We note that the conversion efficiency of thermoelectric devices is measured by the so-called figure of merit $ZT = S^2 \sigma T / \kappa$. Here, the combination $S^2 \sigma$ of the Seebeck coefficient S and the conductivity σ is called the power factor (PF), and κ is the thermal conductivity. The power factor of FeSi, displayed in Fig. 4B, peaks at around 60 K, where it reaches more than $40 \mu\text{W}/(\text{K}^2 \text{cm})$ (i.e., it reaches values comparable to state-of-the-art Bi₂Te₃, at its maximum value at 550 K), and is for $T \geq 60$ K larger than in FeSb₂, which holds the overall record PF (realized at 12 K) (3).

Microscopic Insights

The quantitative agreement of our theoretical results with a large panoply of experimental data validates our approach, thus signaling the paramount influence of electronic correlation effects. Drawing from the microscopic insights of our method, we now address the physical picture underlying the intriguing properties of FeSi, which will, in particular, allow us to propose ways to improve the thermoelectrical properties of FeSi.

Cross-Over to the Metallic State. Within our theoretical picture, the cross-over to bad metallic behavior is not caused by a narrowing of the excitation gap (see *SI Text* for details). Instead, it is filled with incoherent weight that emerges with increasing temperature. Information about the coherence of the one-particle excitations

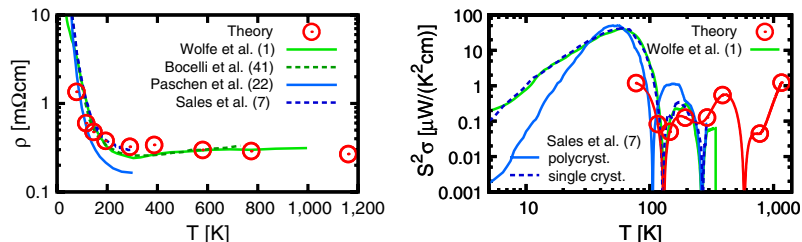


Fig. 4. Resistivity and power factor. (A) Shown is a comparison of the theoretical resistivity of FeSi with several experimental results (1, 7, 22, 41). (B) The power factor of FeSi, theory in comparison with experimental data compiled from refs. 1 and 7.

are encoded in the imaginary parts of the electron self-energy Σ . For the relevant orbital components we find $\Im\Sigma(\omega = 0) \approx -aT^2$ with $a = 1.9 \times 10^{-4} \text{ meV/K}^2$. $\Im\Sigma$ thus reaches the value of $\Delta/2$ at around 400 K, when only a pseudogap remains (see Fig. 1).

Complementarily, it was proposed that the arguably large electron–phonon coupling (7, 11, 24) causes the closure of the gap via thermal-induced atomic disorder (10, 11). In molecular dynamics simulations (11), the gap Δ_{DFT} was shown to vanish abruptly for temperatures of the order of $T \approx \Delta_{\text{DFT}}/2$, in contrast to the gradual transition that is observed in experiment and reproduced by our theory. We note also that, in other systems with large electron–phonon coupling, spectral weight transfers are quantitatively accounted for by electronic correlations (33).

Strength of Correlations. A recurring question in condensed matter physics is whether a system is well described in either an itinerant or a localized picture. Both the low effective mass of FeSi ($m^*/m \approx 1.5$) and the rather high kinetic energy $E_{\text{kin}} \approx -10.5 \text{ eV}$ of the iron states signal a large degree of delocalization. Indeed, other iron compounds show significantly higher masses and lower kinetic energies, e.g., the pnictides BaFe_2As_2 ($E_{\text{kin}}[\text{eV}]; (m^*/m)_{xy}) \approx (-7; 3)$ and CaFe_2As_2 ($-8; 2.5$) or the chalcogen FeTe ($-6.5; 7$) (34). Accordingly, FeSi is an only moderately correlated, itinerant material. Yet effects of correlation-induced incoherence are essential for the cross-over to the metallic state. This seeming contradiction is resolved by noting that all relevant energy scales are of similar magnitude. Indeed, $\mathcal{O}(\Delta) \approx \mathcal{O}(\Im\Sigma) \approx \mathcal{O}(T) \approx \mathcal{O}(50 \text{ meV})$, which leads low-energy properties to be correlation dominated.

The Spin State. A major signature of the unconventional behavior of FeSi is the nonmonotonous uniform magnetic susceptibility (5). The latter is closely mimicked by our local spin susceptibility $\chi_{\text{loc}}(\omega = 0) \sim \frac{1}{\beta} \int d\tau \langle S_z(\tau) S_z(0) \rangle$ (see inset of Fig. 1), indicating compatibility with the picture of electronic correlations. Interestingly there is a distinction of timescales: Whereas $\chi_{\text{loc}}(\omega = 0)$ —the time-averaged response—displays a strong temperature de-

pendence, the spin response at very short timescales, as probed by the observable $\lim_{\tau \rightarrow 0} \langle S(\tau) S(0) \rangle$, is virtually temperature independent. From the latter, we obtain an effective moment $M = \sqrt{S(S+1)}g_s \approx 3(g_s = 2)$, which is consistent with major contributions from effective iron states with $S = 1$ (see *SI Text* for details), and in agreement with $M = 2.7$ as obtained from fitting the experimental susceptibility (5) to a Curie–Weiss law $\chi = \frac{\mu_0 \mu_B}{3k_B} M^2 / (T - T_C)$ for $T > 400 \text{ K}$. We note that the local susceptibility (see inset of Fig. 1) is about one order of magnitude smaller than the experimental uniform susceptibility. Hence, the temperature-induced fluctuating moment of the underlying spin state is, to a large extent, not local. The nonlocality is corroborated by neutron experiments (35) that find a significant magnetic scattering at “ferromagnetic” reciprocal lattice vectors.

Because the effective moment M is constant, FeSi thus does not undergo a spin-state transition as is found, e.g., in MnO or LaCoO_3 . There it originates from a competition between the Hund’s coupling J and the crystal field splittings. In FeSi, the splitting of low-energy excitations is given by the gap Δ , which is much smaller than the Hund’s coupling J , thereby favoring the high spin configuration.

The preponderance of $S = 1$ states, in particular, implies that FeSi is not a singlet insulator as previously proposed (16, 17). We further find that FeSi is in a mixed valence state. We obtain an iron valence of $N_d \approx 6.2$, with a large variance $\delta N = \langle (N - \langle N \rangle)^2 \rangle \approx 0.93$ (see *SI Text* for details). However, these numbers are insensitive to temperature, thus excluding a thermally induced mixed valence (18).

Interestingly, we find that our results are one order of magnitude more sensitive to the strength of the Hund’s rule coupling J than to the Hubbard interaction U (for details, see *SI Text*). This effect is reminiscent of the physics of Hund’s metals as found in iron pnictides and chalcogenides (34, 36), and is quite different from Hubbard physics in which the Hubbard U reduces charge fluctuations and the timescale associated with them, while the time-averaged local spin susceptibility is strongly enhanced. In contrast, only the spin fluctuations (but not the charge fluctuations) are short-lived in FeSi, resulting in only a moderate enhancement of the (time-averaged) local spin susceptibility, but a strongly enhanced short time (energy-averaged) fluctuating magnetic moment.

The Physical Picture

We are now in the position to elucidate the fundamental picture of FeSi: (i) What is the physical origin of the cross-over in the susceptibility? (ii) How is the latter linked to the emergence of incoherent spectral weight—i.e., what is the relation between the cross-overs for the spin and charge degrees of freedom?

At low temperatures, FeSi is a conventional band-like semiconductor; i.e., it is approximately described by an effective one-particle Hamiltonian that can be diagonalized in momentum space. Excitations are well defined (coherent). The system is in a high spin state, but spin excitations are gapped, and so the spin susceptibility is small as fluctuations at finite timescales are quenched. In this sense, the spin degrees of freedom are inactive.

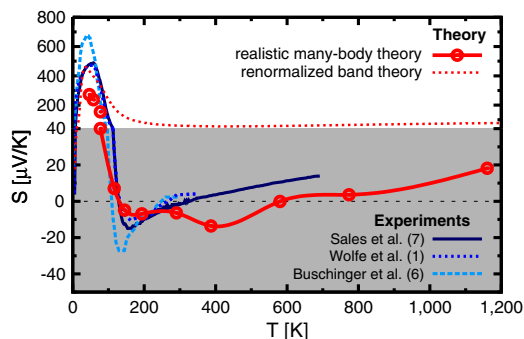


Fig. 5. Thermopower. Theoretical Seebeck coefficient in comparison with experiments (1, 6, 7). Note the change in scale above $40 \mu\text{V/K}$. The line connecting the many-body theory results is a guide to the eye. The unconnected points at low temperature are obtained from an analysis of the asymptotic behavior of the many-body calculation.

With increasing temperature, however, a fluctuating moment develops at the iron sites. The emergence of such a locking to the real-space lattice breaks down the momentum-space description: k is no longer a good quantum number, hence excitations acquire a finite lifetime broadening, and the spectrum becomes incoherent.

Our theory goes beyond previous theoretical proposals, indeed it reconciles (and validates by including explicitly the Si degrees of freedom) two seminal model-based approaches: The model of Fu and Doniach (12) that addressed the evolution of the one-particle spectrum, and which can serve as a simplified cartoon of our realistic calculation, and the spin-fluctuation theory of Takahashi and Moriya (13), which is compatible with our results for the spin degrees of freedom. Here, we claim that the cross-overs in the spin and charge response are actually intimately linked to each other.

Due to the complicated multiorbital nature of the problem, there are however important differences from previous model calculations (12, 14, 15): In the realistic case, the relevant control parameter is the Hund's coupling J rather than the Coulomb interaction U (see *SI Text*). Furthermore, we account for the particle/hole asymmetry. Indeed, for a symmetric model (12), the Seebeck coefficient—a key feature of this system—is zero at all temperatures, and the chemical potential is pinned to its value at 0 K.

Conclusions and Outlook

To summarize, we have obtained a fundamental microscopic theory of iron silicide, the canonical example of a correlated insulator. This material features a competitive power factor in the temperature range of 50–100 K. Our theory suggests concrete ways to improve that already remarkable thermoelectric perfor-

mance. First, as is becoming standard practice in thermoelectric development (37), nano- or heterostructuring is needed to reduce thermal conductivity to convert the good power factor into a large figure of merit. More important yet, the power factor can be improved further by increasing the charge gap, through a reduction of the ratio of Hund's coupling over bandwidth, or an increase in the interatomic hybridizations that cause the band gap. To achieve this goal, we propose experimental studies of FeSi under external pressure (38) or by compressing the lattice using a suitable substrate. A particularly interesting option would be partial isoelectronic substitution of iron with ruthenium (39). Not only does the isostructural RuSi have a larger gap than FeSi, and itself a notable Seebeck coefficient above 100 K (40), but also the fluctuating moment physics that drives the metalization and the quenching of the thermopower in FeSi could be effectively reduced, as well as the thermal conductivity decreased via the alloying. To our knowledge these avenues have not been pursued vis-à-vis their impact onto thermoelectricity. More generally, the theory outlined here describes the subtle interplay of electron–electron correlations and thermoelectricity, adding another host of systems amenable to theory-assisted thermoelectric material design.

ACKNOWLEDGMENTS. We thank P. Sun and F. Steglich for interesting discussions as well as for sharing unpublished results. The authors were supported by the National Science Foundation (NSF) materials world network under Grants NSF DMR 0806937 and NSF DMR 0906941, and by the Partner University Fund program. Acknowledgment is also made to the donors of the American Chemical Society Petroleum Research Fund 48802 for partial support of this research.

- Wolfe R, Wernick JH, Haszko SE (1965) Thermoelectric properties of FeSi. *Phys Lett* 19:449–450.
- Schlesinger Z, et al. (1993) Unconventional charge gap formation in FeSi. *Phys Rev Lett* 71:1748–1751.
- Bentien A, Johnsen S, Madsen GKH, Iversen BB, Steglich F (2007) Colossal Seebeck coefficient in strongly correlated semiconductor FeSb₂. *Europhys Lett* 80:17008.
- Bittar EM, Capan C, Seyfarth G, Pagliuso PG, Fisk Z (2010) Correlation effects in the small gap semiconductor FeGa₃. *J Phys Conf Ser* 200:012014.
- Jaccarino V, Wertheim GK, Wernick JH, Walker LR, Araj S (1967) Paramagnetic excited state of FeSi. *Phys Rev* 160:476–482.
- Buschinger B, et al. (1997) Transport properties of FeSi. *Phys B* 230–232:784–786.
- Sales BC, Delaire O, McGuire MA, May AF (2011) Thermoelectric properties of Co-, Ir-, and Os-doped FeSi alloys: Evidence for strong electron-phonon coupling. *Phys Rev B Condens Matter Mater Phys* 83:125209.
- Sun P, Oeschler N, Johnsen S, Iversen BB, Steglich F (2010) Narrow band gap and enhanced thermoelectricity in FeSb₂. *Dalton Trans* 39:1012–1019.
- Tomczak JM, Haule K, Miyake T, Georges A, Kotliar G (2010) Thermopower of correlated semiconductors: Application to FeAs₂ and FeSb₂. *Phys Rev B Condens Matter Mater Phys* 82:085104.
- Jarlborg T (1999) Electronic structure and properties of pure and doped ϵ -FeSi from ab initio local-density theory. *Phys Rev B Condens Matter Mater Phys* 59:15002–15012.
- Delaire O, et al. (2011) Phonon softening and metallization of a narrow-gap semiconductor by thermal disorder. *Proc Natl Acad Sci USA* 108:4725–4730.
- Fu C, Doniach S (1995) Model for a strongly correlated insulator FeSi. *Phys Rev B Condens Matter Mater Phys* 51:17439–17445.
- Takahashi Y, Moriya T (1979) A theory of nearly ferromagnetic semiconductors. *J Phys Soc Jpn* 46:1451–1459.
- Mazurenko VV, et al. (2010) Metal-insulator transitions and magnetism in correlated band insulators Fes_{1-x}Co_xSi. *Phys Rev B Condens Matter Mater Phys* 81:125131.
- Kuneš J, Anisimov VI (2008) Temperature-dependent correlations in covalent insulators: Dynamical mean-field approximation. *Phys Rev B Condens Matter Mater Phys* 78:033109.
- Anisimov VI, Ezhov SY, Elfimov IS, Solovoyev IV, Rice TM (1996) Singlet semiconductor to ferromagnetic metal transition in FeSi. *Phys Rev Lett* 76:1735–1738.
- van der Marel D, Damascelli A, Schulte K, Menovsky AA (1998) Spin, charge, and bonding in transition metal mono-silicides. *Phys B* 244:138–147.
- Varma CM (1994) Aspects of strongly correlated insulators. *Phys Rev B Condens Matter Mater Phys* 50:9952–9956.
- Kotliar G, et al. (2006) Electronic structure calculations with dynamical mean-field theory. *Rev Mod Phys* 78:865–951.
- Haule K, Yee CH, Kim K (2010) Dynamical mean-field theory within the full-potential methods: Electronic structure of CeIrIn₅, CeCoIn₅, and CeRhIn₅. *Phys Rev B Condens Matter Mater Phys* 81:195107.
- De Giorgi L, et al. (1994) Optical evidence of Anderson-Mott localization in FeSi. *Europhys Lett* 28:341–346.
- Paschen S, et al. (1997) Low-temperature transport, thermodynamic, and optical properties of FeSi. *Phys Rev B Condens Matter Mater Phys* 56:12916–12930.
- Damascelli A, Schulte K, van der Marel D, Menovsky AA (1997) Infrared spectroscopic study of phonons coupled to charge excitations in FeSi. *Phys Rev B Condens Matter Mater Phys* 55:R4863–R4866.
- Menzel D, et al. (2009) Electron-phonon interaction and spectral weight transfer in Fe_{1-x}Co_xSi. *Phys Rev B Condens Matter Mater Phys* 79:165111.
- Rozenberg MJ, Kotliar G, Kajuter H (1996) Transfer of spectral weight in spectroscopies of correlated electron systems. *Phys Rev B Condens Matter Mater Phys* 54:8452–8468.
- Mattheiss LF, Hamann DR (1993) Band structure and semiconducting properties of FeSi. *Phys Rev B Condens Matter Mater Phys* 47:13114–13119.
- Klein M, et al. (2008) Evidence for itineracy in the anticipated kondo insulator FeSi: A quantitative determination of the band renormalization. *Phys Rev Lett* 101:046406.
- Arita M, et al. (2008) Angle-resolved photoemission study of the strongly correlated semiconductor FeSi. *Phys Rev B Condens Matter Mater Phys* 77:205117.
- Mahan GD, Sofo JO (1996) The best thermoelectric. *Proc Natl Acad Sci USA* 93:7436–7439.
- Sakai A, et al. (2007) Thermoelectric power in transition-metal monosilicides. *J Phys Soc Jpn* 76:093601.
- Saso T, Urasaki K (2002) Seebeck coefficient of kondo insulators. *J Phys Soc Jpn* 71:288–290.
- Oudovenko VS, Kotliar G (2002) Thermoelectric properties of the degenerate Hubbard model. *Phys Rev B Condens Matter Mater Phys* 65:075102.
- Tomczak JM, Biermann S (2009) Optical properties of correlated materials: Generalized Peierls approach and its application to VO₂. *Phys Rev B Condens Matter Mater Phys* 80:085117 arXiv:0904.3388.
- Yin ZP, Haule K, Kotliar G (2011) Kinetic frustration and the nature of the magnetic and paramagnetic states in iron pnictides and iron chalcogenides. *Nat Mater* 10:932–935.
- Shirane G, Fischer JE, Endoh Y, Tajima K (1987) Temperature-induced magnetism in FeSi. *Phys Rev Lett* 59:351–354.
- Haule K, Kotliar G (2009) Coherence-incoherence crossover in the normal state of iron oxypnictides and importance of Hund's rule coupling. *New J Phys* 11:025021.
- Snyder GJ, Toberer ES (2008) Complex thermoelectric materials. *Nat Mater* 7:105–114.
- Bauer E, Bocelli S, Hauser R, Marabelli F, Spolenak R (1997) Stoichiometric effects on the optical spectra and pressure response of Fe_{1-x}Mn_xSi. *Phys B* 230–232:794–796.
- Mani A, et al. (2002) Evolution of the Kondo insulating gap in Fe_{1-x}Ru_xSi. *Phys Rev B Condens Matter Mater Phys* 65:245206.
- Hohl H, Ramirez A, Goldmann C, Ernst G, Bucher E (1998) Transport properties of RuSi, RuGe, OsSi, and quasi-binary alloys of these compounds. *J Alloys Compd* 278:39–43.
- Bocelli S, Marabelli F, Spolenak R, Bauer E (1996) Evolution of the optical response from a very narrow gap semiconductor to a metallic material in Fe_{1-x}Mn_xSi. *Mat Res Soc Symp Proc* 402:361–366.